Circulation and Variability over the Meso-American Barrier Reef System: Application of a Triply Nested Ocean Circulation Model

Jinyu Sheng[1]

Abstract

A triply nested-grid ocean circulation modeling system is used to simulate the circulation and associated seasonal variability on the Meso-American Barrier Reef System (MBRS) of the northwest Caribbean Sea. The nested-grid system consists of three subcomponents: a coarse-resolution outer model of the western Caribbean Sea (WCS); an intermediate-resolution middle model of the southern Meso-American Barrier Reef System; and a fine-resolution inner model of the Belizean shelf. The two-way nesting technique based on the smoothed semi-prognostic method developed by Sheng et al. (2005) is used to exchange information between the three subcomponents of the system. The nested-grid system is forced by 12-hourly NCEP wind and climatological monthly mean sea surface heat and freshwater fluxes and integrated for 11 years from 1990 to 2000. Model results of the last 10 years are used to calculate the monthly mean currents, temperature/salinity distributions and associated variability over the MBRS. Model results demonstrate that the circulation has significant temporal and spatial variability in the study region.

[1]Department of Oceanography, Dalhousie University, Halifax, Nova Scotia, Canada, B3H 4J1; phone: 902-494-2718; Email: Jinyu.Sheng@Dal.Ca

Introduction

The main objective of this study is to examine the three-dimensional circulation and associated seasonal variability on the Meso-American Barrier Reef System (MBRS) of the northwestern Caribbean Sea, using a triply nested-grid ocean circulation modeling system. MBRS extends 1000 km from the Bay Islands of Honduras through Guatemala and Belize to the tip of Mexico's Yucatan peninsula. Reef ecosystems are the marine equivalents of terrestrial rainforests in terms of biodiversity (Hubbell, 1997), and have significant economic values in terms of exploited resources, waste disposal, protection of coastal property and as a basis for tourism. The coral reefs and associated lagoons on the MBRS serve as important habitat, breeding and feeding grounds for a great diversity of marine invertebrates, fish, reptiles and mammals (Kramer and Kramer, 2002). Reefs of the MBRS have been affected significantly by natural and anthropogenic factors including hurricanes, disease outbreaks, coral bleaching, and various disturbances and stresses resulting from human activities in the region over the last 30 years. There is thus an increasing demand for better understanding of physical, ecological and biological processes that connect and sustain the marine ecosystems of the MBRS.

Several numerical studies were made in the past to examine the general circulation and variability on the MBRS. Readers are referred to Oey et al. (2005) for a review of numerical models of the MBRS. Sou et al. (1996) simulated the general circulation in the western Caribbean Sea (WCS) using the Modular Ocean Model, with a coarse resolution of about 55 km. Sheng and Tang (2003) studied the circulation in the western Caribbean Sea using a limited-area, single-domain ocean circulation model, with a horizontal resolution of about 18 km. Sheng and Tang (2004) studied the circulation over the MBRS using a two-level nested-grid model with a fine-resolution (about 6 km) inner model imbedded inside the coarse-resolution western Caribbean Sea developed earlier by the authors (Sheng and Tang, 2003). Ezer et al. (2005) examined the variability of the currents over MBRS using a high-resolution circulation model based on the Princeton Ocean Model with a variable horizontal resolution ranging from 3 km along the MBRS to 8 km on the open eastern boundary. Tang et al. (2006) recently examined the circulation and hydrodynamic connectivity of surface waters on the Belize shelf (BS) using a nested-grid model. All of these studies use the monthly mean wind forcing to drive the model. In this paper we examine the general circulation and seasonal variability on the MBRS using a triply nested-grid ocean circulation modeling system forced by 6-hourly NCEP winds and monthly mean sea surface heat and freshwater fluxes.

The remainder of the paper is arranged as follows. The paper first describes the nested-grid ocean circulation modeling system and the two-way nesting technique. It then presents the monthly mean circulation and seasonal variability in the MBRS during a 10 year period from 1991 to 2000. The final section is a summary.

The Nested-Grid Ocean Circulation Modeling System

This study uses the triply nested-grid ocean circulation modeling system developed by Tang et al. (2006) based upon the Canadian version of Diecast (CANDIE), which is a three-dimensional (3D) ocean circulation model developed by Sheng et al. (1998). The nested-grid modeling system of the MBRS has three subcomponents (Figure 1): (a) a coarse-resolution (~19 km) outer model covering the WCS (72^{o}W-90^{o}W, 8^{o}N-25^{o}N); (b) a moderate-resolution (~6.2 km) middle model covering the southern MBRS (84^{o}W-89^{o}W, 15.5^{o}N-19.4^{o}N); and (c) a fine-resolution (~2.1 km) inner model covering the BS (87.3^{o}W–88.43^{o}W, 16.1^{o}N–17.98^{o}N). The three subcomponents have the same 28 unevenly spaced z-levels in the vertical, with the centers of each z-level located respectively at 1, 3, 5, 7, 9, 11, 13, 15, 17, 19, 25, 40, 75, 140, 230, 340, 450, 575, 725, 900, 1250, 1750, 2250, 2750, 3250, 3750, 4250, and 4750 m. The system uses the digital bathymetry database of 2-minute resolution (DBDB2) developed by the Ocean Dynamics and Prediction Branch, the Naval Research Laboratory of the United States (Dong-Shan Ko, personal communication, 2003). In comparison with the model setup in Tang et al., (2006), the model setup in this study has slightly smaller middle and inner model domains (to speed up model integrations), a higher vertical resolution in the top 100 m (to better resolve the shelf circulation on the MBRS), and lower vertical resolution below 1000 m.

The nested-grid system of the MBRS uses the vertical mixing scheme of Large et al. (1994) for vertical eddy viscosity and diffusivity coefficients K_m and K_h, and the horizontal mixing scheme of Smagorinsky (1963) for the horizontal eddy viscosity coefficient A_m, with the horizontal turbulent Prandtl Number A_h/A_m set to 0.1, where A_h is the horizontal eddy diffusivity coefficient. Since the Smagorinsky scheme is resolution dependent, it has the desirable effect of having different levels of horizontal mixing in the different subcomponents of the nested-grid system. The nested-grid system also uses the fourth-order numerics suggested by Dietrich (1997) and the flux limiter developed by Thuburn (1996) to better represent the nonlinear advection terms in the model.

The nested-grid system uses the two-way nesting technique based on the smoothed semi-prognostic (SSP) method developed by Sheng et al. (2005). Readers are

referred to Sheng et al. (2001) and Greatbatch et al. (2004) for the semi-prognostic method and Sheng et al. (2005) for the SSP nesting technique. Only a brief summary is provided here. The application of the SSP two-way nesting technique includes the following three steps. First, the middle model temperature and salinity are interpolated onto the inner model grid to adjust the momentum equation of the inner model over the common sub-region where the inner and middle model grids overlap based on

$$\frac{\partial p_{inn}}{\partial z} = -g\rho_{inn} - g(1-\beta_{inn})\langle \hat{\rho}_{mid} - \rho_{inn} \rangle \tag{1}$$

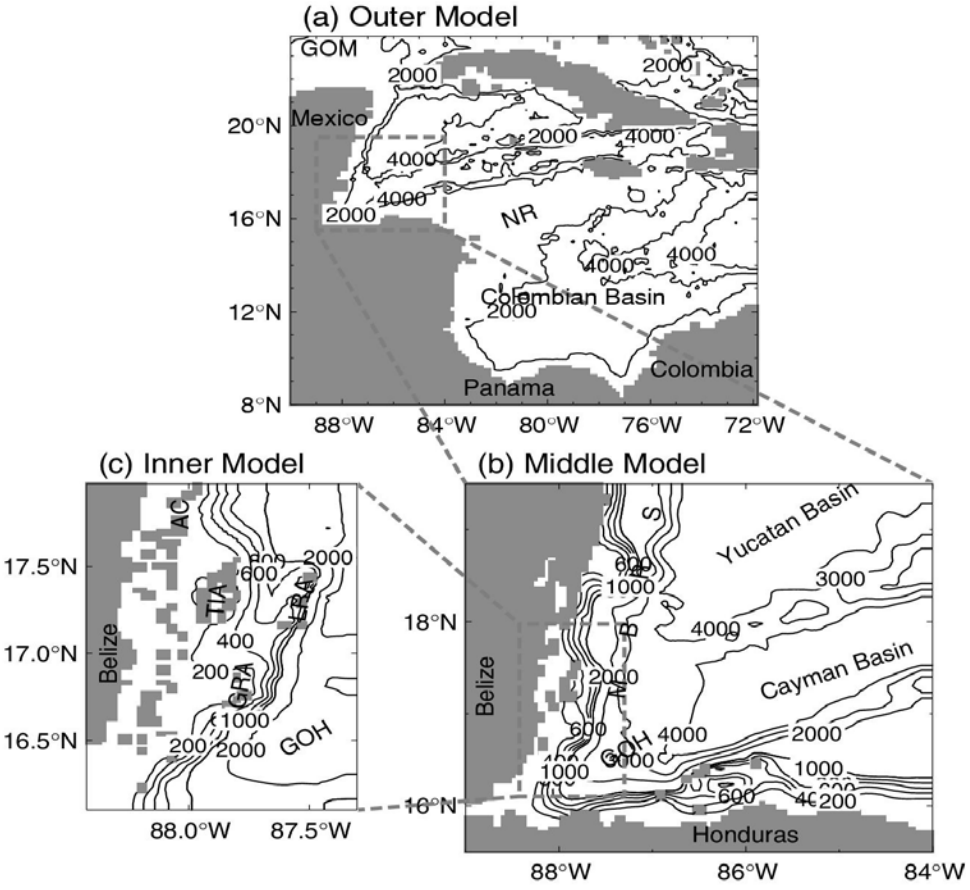

Figure 1. Selected bathymetric features for (a) an outer model covering the western Caribbean Sea; (b) a middle model covering the southern and central Meso-American Barrier Reef System (MBRS); and (c) an inner model covering the Belize shelf. Abbreviations are used for Lighthouse Reef Atoll (LRA), Turneffe Islands Atoll (TIA), Glovers Reef Atoll (GRA), Ambergris Cay (AC), Nicaragua Rise (NR), Gulf of Hunduras (GOH), and Gulf of Mexico (GOM). Contours are labeled in units of meters.

where p_{inn} and ρ_{inn} are respectively pressure and density variables of the inner model, $\hat{\rho}_{mid}$ is density calculated from the middle model temperature and salinity after interpolation onto the inner model grid, β_{inn} is the linear combination coefficient with a value between 0 and 1, and $\langle\ \rangle$ is a filtering operator. The filtering operator ensures that the inner model is constrained by the middle model only on large scales, the smaller scales associated with the fine grid of the inner model being free to evolve.

Second, the middle model temperature and salinity are interpolated onto the outer model grid to adjust the momentum equations of the outer model over the common sub-region where the outer and middle model grids overlap, based on

$$\frac{\partial p_{out}}{\partial z} = -g\rho_{out} - g(1-\beta_{out})\langle\tilde{\rho}_{mid} - \rho_{out}\rangle \tag{2}$$

where p_{out} and ρ_{out} are respectively pressure and density variables of the outer model, $\tilde{\rho}_{mid}$ is density calculated from middle model temperature and salinity after interpolation onto the outer model grid, β_{out} is the linear combination coefficient with a value between 0 and 1, and $\langle\ \rangle$ is the filtering operator, which usually differs from that in Eq. (1).

Third, the outer and inner model temperature and salinity are interpolated onto the middle model grid to adjust the momentum equation of the middle model over the overlapping sub-region, based on

$$\frac{\partial p_{mid}}{\partial z} = -g\rho_{mid} - g(1-\beta_{mid})\langle\hat{\rho}_{opi} - \rho_{mid}\rangle \tag{3}$$

where p_{mid} and ρ_{mid} are pressure and density variables of the middle model respectively, $\hat{\rho}_{opi}$ is density calculated from the outer and inner model temperature and salinity after interpolation onto the middle model grid, and β_{mid} is the linear combination coefficient with a value between 0 and 1.

In this study, we follow Sheng et al. (2005) and set the linear combination coefficients β_{inn}, β_{out} and β_{mid} to 0.5. Readers are referred to Sheng et al. (2005) for sensitivity studies of mode results to different values of these coefficients. The filtering operator used in this study is the running averaging, with a smoothing scale of 24 km for the inner model, and 72 km for the middle model. The filtering operator in (3) for the outer model is not used.

The following boundary conditions are used in the three sub-components of the nested-grid system. At lateral closed boundaries, the normal flow, tangential stress

of the currents and horizontal fluxes of temperature and salinity are set to zero. Along open boundaries, the normal flow, temperature and salinity fields are calculated using adaptive open boundary conditions (Marchesiello et al., 2001). It first uses an explicit Orlanski (1976) radiation condition to determine whether the open boundary is passive or active. If the open boundary is passive, the model prognostic variables are radiated outward to allow perturbations generated inside the model domain to propagate outward. If the open boundary is active, the outer model prognostic variables at the open boundary are restored to the monthly mean climatology with a restoring time scale of 15 days, and the middle and inner model prognostic variables at the open boundary are restored to the outer and middle model results respectively, with a restoring time scale of 5 hours. In addition, the depth-mean normal flows across the outer model open boundaries are set to be the monthly mean results produced by a $(1/3)^o$ Atlantic model based on FLAME (Family of Linked Atlantic Model Experiments).

The nested-grid system is initialized with January mean climatology of temperature and salinity, and integrated for 11 years from January 1, 1990 to December 31, 2000 with 6 hourly wind stresses and climatological monthly mean surface heat flux. The wind stresses are converted from NCEP wind speeds using the bulk formula of Large and Pond (1981). The horizontal resolution of NCEP reanalysis fields is about 200 km in the WCS.

Figure 2 shows the monthly mean wind stresses in February, May, August and November calculated from 6 hourly NCEP wind stresses during a 10-year period from 1991 to 2000. These monthly-mean wind stresses are used to represent the surface wind forcing in four different seasons during the 10-year period. The monthly mean wind stress in February is roughly southwestward in the WCS, which is relatively stronger (about 1.0 to 1.4 dyn cm^{-2}) over the southern Colombian Basin and eastern Yucatan Basin, and relatively weaker (~0.5 dyn cm^{-2}) over the MBRS and Cayman Basin. In May and August, the monthly mean wind stress is nearly westward over the WCS and stronger (~1.2 dyn cm^{-2}) over the central Colombian Basin and relatively weaker (~0.5 dyn cm^{-2}) over the Cayman and Yucatan Basins. In November, the monthly mean wind stress is approximately westward over the Colombian Basin and southwestward over the Cayman and Yucatan Basins, which is relatively stronger (~1.5 dyn cm^{-2}) over the central Colombian Basin and eastern Cayman and Yucatan Basins (~0.9 dyn cm^{-2}) and relatively weaker over the MBRS (~0.5 dyn cm^{-2}). Figure 2 also demonstrates that the monthly mean wind stress over the MBRS is relatively stronger in February and November and weaker in May and August.

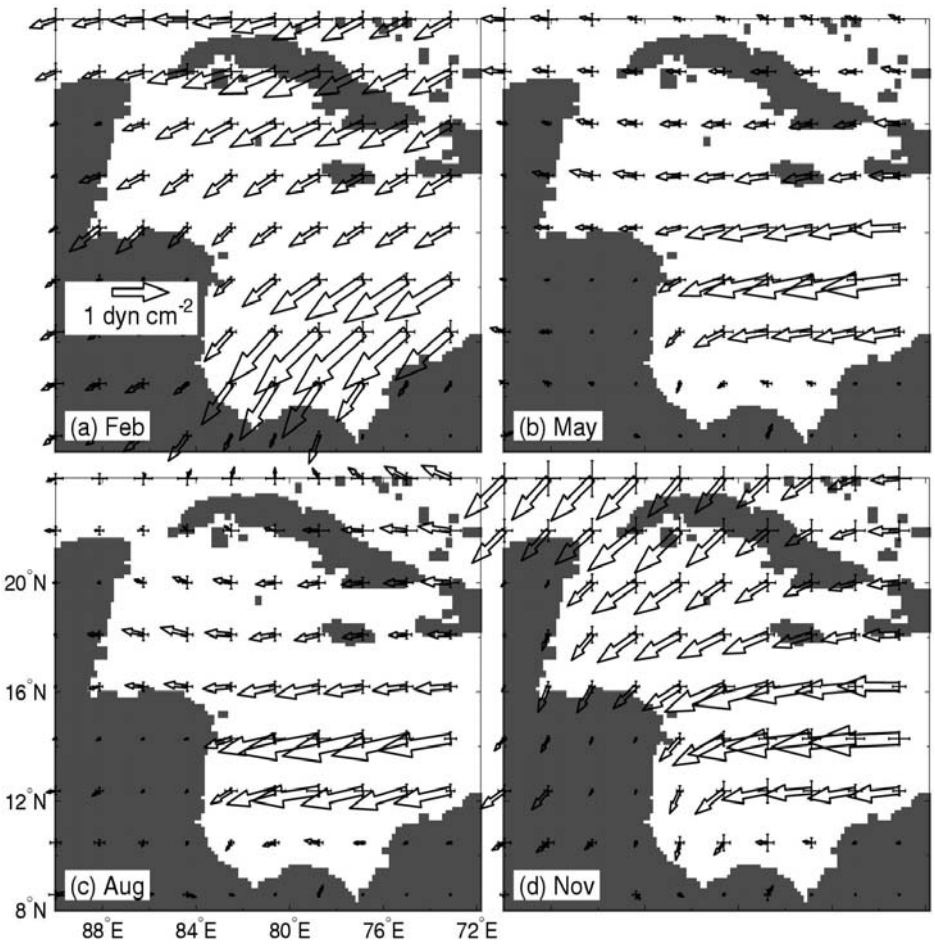

Figure 2. Monthly mean wind stresses in (a) February; (b) May; (c) August; and (c) November calculated from 6 hourly NCEP wind forcing during a 10-year period from 1991 to 2000.

The net heat flux through the sea surface (Q_{net}) is expressed as (Barnier et al., 1995):

$$Q_{net} = Q_{\text{net}}^{\text{clim}} + \gamma(SST^{\text{clim}} - SST^{\text{model}}) \qquad (4)$$

where $Q_{net}^{c\lim}$ is the monthly mean net heat flux taken from da Silva et al. (1994), $SST^{c\lim}$ is the monthly mean sea surface temperature, and γ is the coupling coefficient defined as $\Delta z_1 \rho_0 c_p / \tau_Q$, where Δz_1 is the thickness of the top z-level, c_p the specific heat, and τ_Q the restoring time scale set to 15 days. The implied value of γ is about 35 W m^{-2} K^{-1}, which is comparable to values calculated from observations (Haney, 1971). We also restore the model sea surface salinity to the monthly mean climatology at a time scale of 15 days.

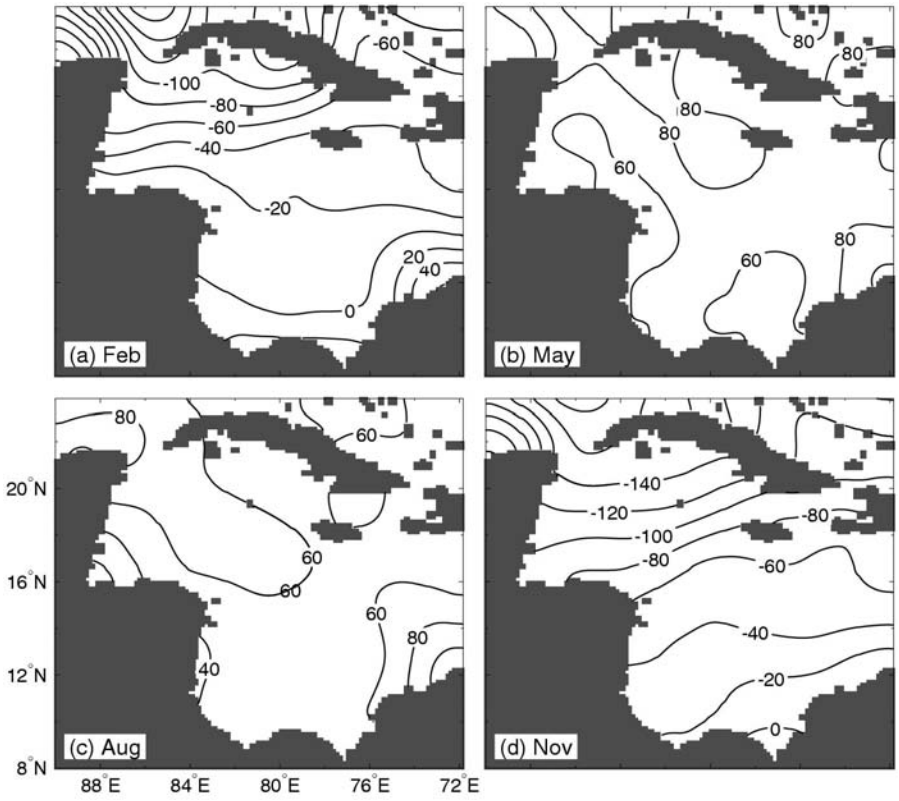

Figure 3. Monthly mean climatology of net surface heat fluxes constructed by da Silva et al. (1994) in (a) February; (b) May; (c) August; and (d) November.

Figure 3 shows the monthly mean heat fluxes of da Silva et al. (1994) in the four months. Except for the coastal regions of Panama and Colombia, the February mean heat fluxes over the WCS are negative (i.e., ocean waters losing heat to the atmosphere), with values of about -20 W m^{-2} over the central and northern Colombian, -40 W m^{-2} over the MBRS and Cayman Basin, and -100 W m^{-2} over the Yucatan Basin. The monthly mean heat fluxes in May and August are positive and relatively uniform over the WCS, ranging from 40 to 80 W m^{-2}. In November, the monthly mean heat fluxes over the WCS are negative, ranging from about -40 W m^{-2} over the Colombian Basin, to -100 W m^{-2} over the Cayman Basin and -140 W m^{-2} over the Yucatan Basin.

Figure 4 shows the monthly mean climatological sea surface temperature (SST) in the four months of February, May, August and November. The 3D monthly mean temperature and salinity climatology in the WCS was constructed from a database compiled by the US National Oceanographic Data Center, using the modified Barnes' algorithm described in Geshelin et al. (1999). The monthly mean SST in the

four months is relatively uniform over the central WCS (including the central and northern Colombian Basin, Cayman basin and central Yucatan Basin), with some small horizontal variations over coastal regions of Colombia and northwestern Cuba. The monthly mean SST in the central WCS is about 26.5^{o}C in February, 27.5^{o}C in May, 28-29^{o}C in August, and 28^{o}C in November. The monthly mean sea surface salinity in the four months (not shown) is about 36.0 ppt over the central WCS, with lower salinity over the coastal regions of Panama, Costa Rica and northwestern Colombia, due mainly to freshwater discharges from the Magdalena River.

The monthly mean temperature and salinity have large horizontal variations below the surface mixed layer. To demonstrate vertical stratifications of temperature and salinity and associated horizontal variations in the WCS, we calculate the domain-averaged vertical profiles of temperature and salinity and associated standard deviations with respect to the domain-averaged values at each depth from the gridded fields in the WCS.

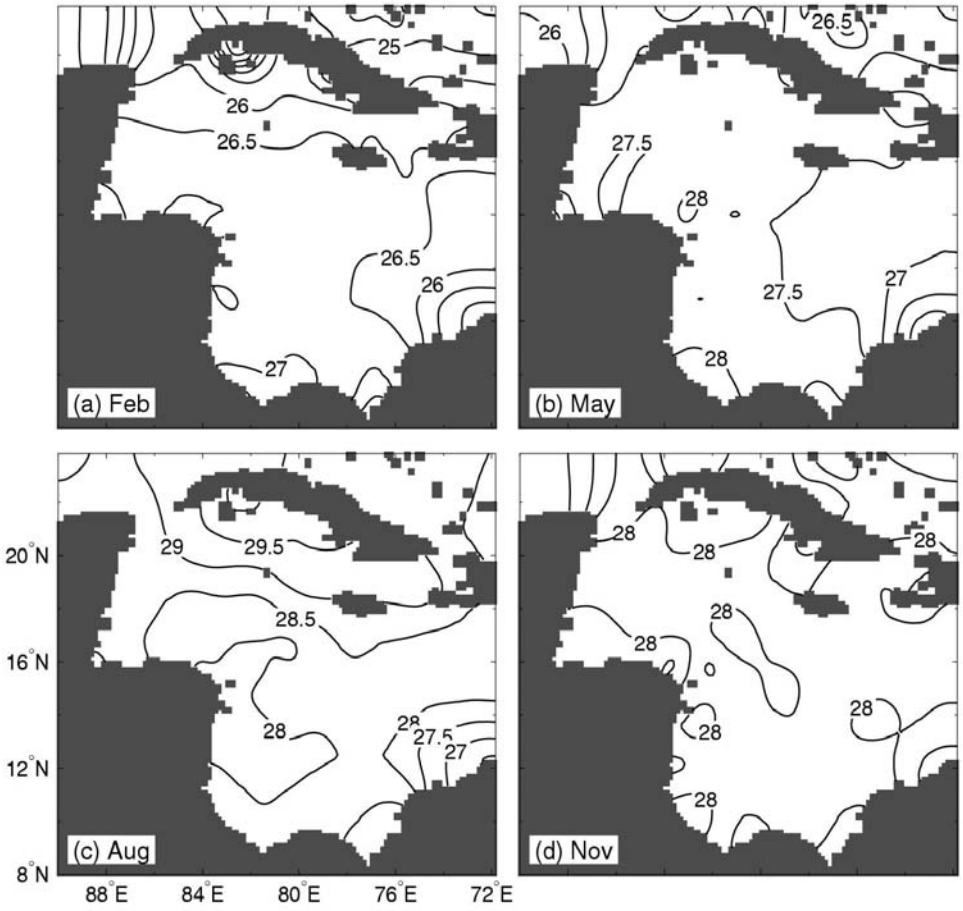

Figure 4. Monthly mean climatology of sea surface temperature in (a) February; (b) May; (c) August; and (d) November.

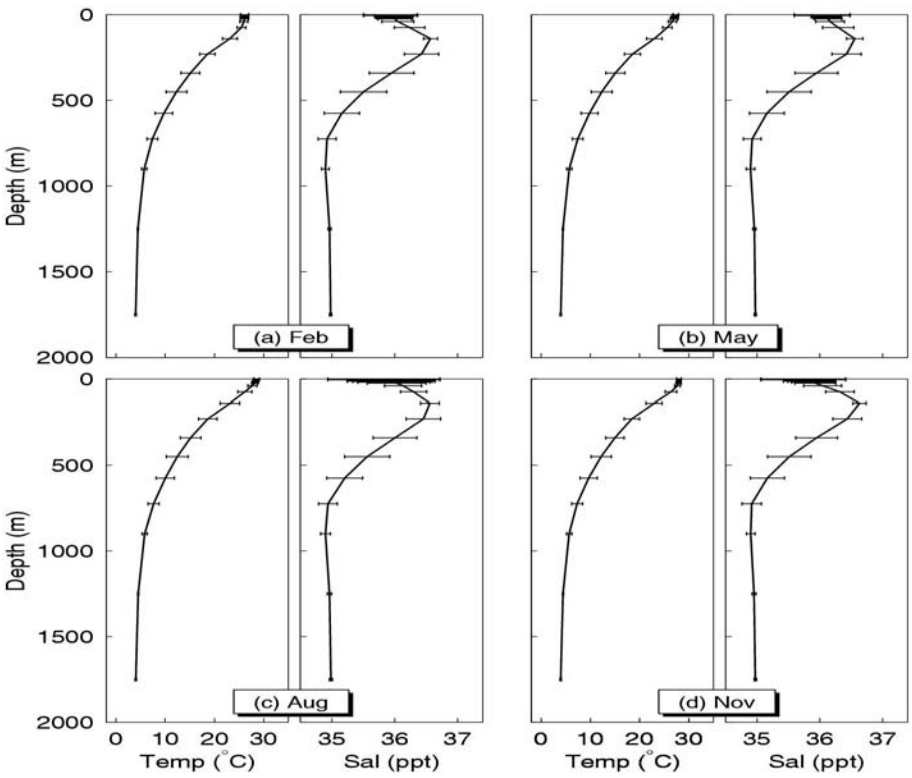

Figure 5. Vertical profiles of domain-averaged climatological monthly mean temperature and salinity in (a) February; (b) May; (c) August; and (d) November. The error bar represents 2 standard deviations with respect to the domain mean at each depth.

Figure 5 demonstrates that vertical profiles of the domain-averaged climatological temperature and salinity in the WCS are very similar in the four months, except for the surface mixed layer. The water column in the WCS has a four-layer vertical structure: a warm and relatively fresh surface mixed layer of less than 100 m; a relatively warm and salty subsurface layer centered at about 200 m; a relatively cold and fresh intermediate layer centered at about 700 m; and a nearly homogeneous deep layer below 2000 m (Mooers and Maul, 1998; Sheng and Tang, 2003). The horizontal variations of the monthly mean temperature in the four months are relatively large at depths from 100 to 1000 m; relatively small in the surface mixed layer; and much weaker below 1000 m. In comparison, the horizontal variations of the monthly mean salinity are relatively large in the surface mixed layer, particularly in summer and autumn months due to larger amounts of freshwater discharges from rivers in the region. The horizontal variations of the monthly mean salinity decrease with depth in top 100 m. After reaching minimum values at about 140 m, the horizontal variations of salinity increase with depth and reach maximum values at

about 400 m. At depths greater than 1000 m, the horizontal variations of climatological monthly mean salinity are relatively small.

Model Results

We integrate the nested-grid system for eleven years from the beginning of 1990 to the end of 2000 and discuss the model results of the last ten years in this paper. Figures 6 and 7 show the instantaneous near-surface (1 m) and sub-surface (450 m) currents and temperature at day 450 (March 26, 1992) produced by the nested-grid system. The near-surface circulation produced by the outer model at this time is characterized by a persistent through flow known as the Caribbean Current, which is relatively broad and roughly westward in the central and eastern Colombian Basin (Figure 6a). The Caribbean Current bifurcates before reaching the Nicaragua Rise, with a weak branch veering southwestward to form the cyclonic, highly variable Panama-Colombia Gyre in the southwestern Caribbean Sea. The main branch of the Caribbean Current turns northwestward and flows along the outer flank of Nicaragua Rise to form a narrow offshore flow running westward and then northward to the Gulf of Mexico. The sub-surface circulation in the WCS at day 450 (Figure 7a) has several large-scale cyclonic gyres in the Colombian Basin, an intense westward flow entering the Cayman Basin from Windward Passage, and strong northwestward flow entering the MBRS from the Colombian Basin through the deep channel between Nicaragua Rise and Jamaica.

The near-surface circulation produced by the intermediate-resolution middle model at day 450 has strong and broad westward currents over the MBRS (Figure 6b). The westward currents bifurcate before reaching the Belize Barrier Reef, with the main branch flowing northward along the eastern coast of Belize, and a small branch flowing southward to the Gulf of Honduras. The sub-surface currents produced by the middle model have a large-scale cyclonic recirculation over the southern MBRS (Figure 7b). A comparison of Figures 6 and 7 demonstrates that the middle model results have similar large-scale circulation features as the outer model results, with more small-scale features resolved by the middle model.

The fine-resolution inner model produces much more small-scale circulation features affected by the local topography over the BS (Figures 6c and 7c), in comparison with the outer and middle model results. The currents produced by the inner model at day 450 are roughly southwestward at 1 m and northward at 450 m on the shelf region and deep waters around Turneffe Islands. The near-surface temperature produced by the inner model is relatively uniform and about 24^{o}C over the deep water, and slightly warmer over the coastal shallow region of the BS.

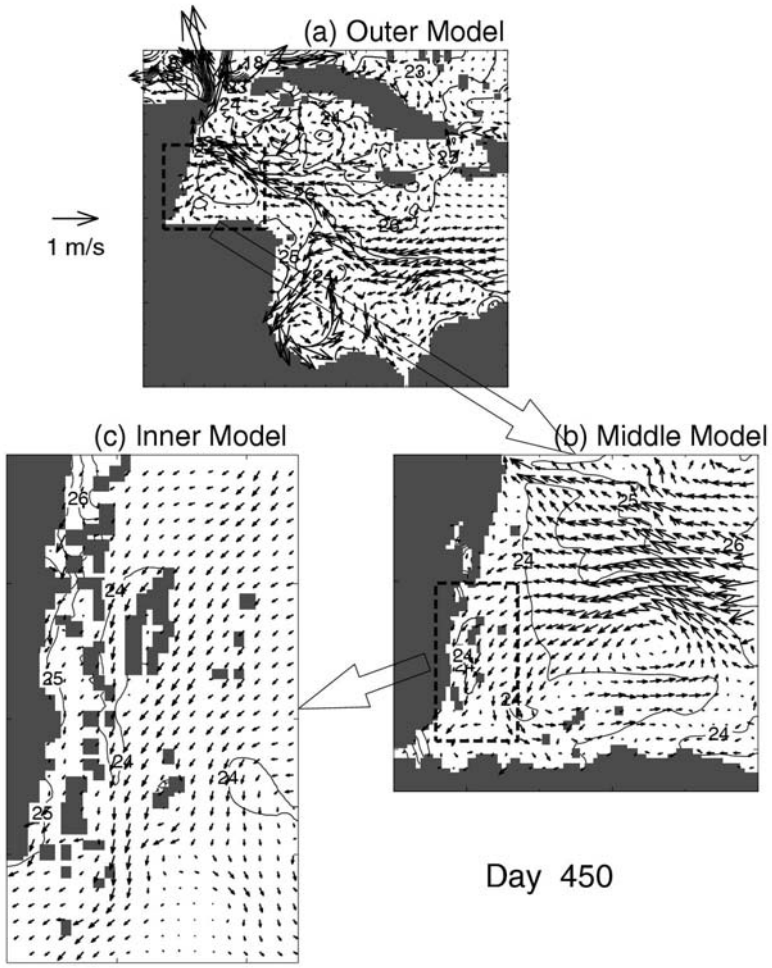

Figure 6. Near-surface (1 m) currents and temperature at day 450 (March 26, 1992) produced by the (a) outer model; (b) middle model, and (c) inner model. Velocity vectors are plotted at every third model grid point.

Figures 8 and 9 present the near-surface (1 m) and sub-surface (450 m) monthly mean currents in February, May, August, and November, calculated from 10-year (1991-2000) results produced by the outer model. The monthly mean currents in the four months are characterized by the persistent Caribbean Current flowing from the eastern Colombian Basin to the western side of the Yucatan Channel and the Panama-Colombia Gyre over the southwestern CS. The Caribbean Current is relatively narrower and stronger in August than in the other three months. The Panama-Colombia Gyre is highly variable, which qualitatively agrees with the previous findings based on the satellite altimetry data (Nystuen and Andrade 1993; Andrade and Barton 2000) and near-surface drifter data (Fratantoni 2001).

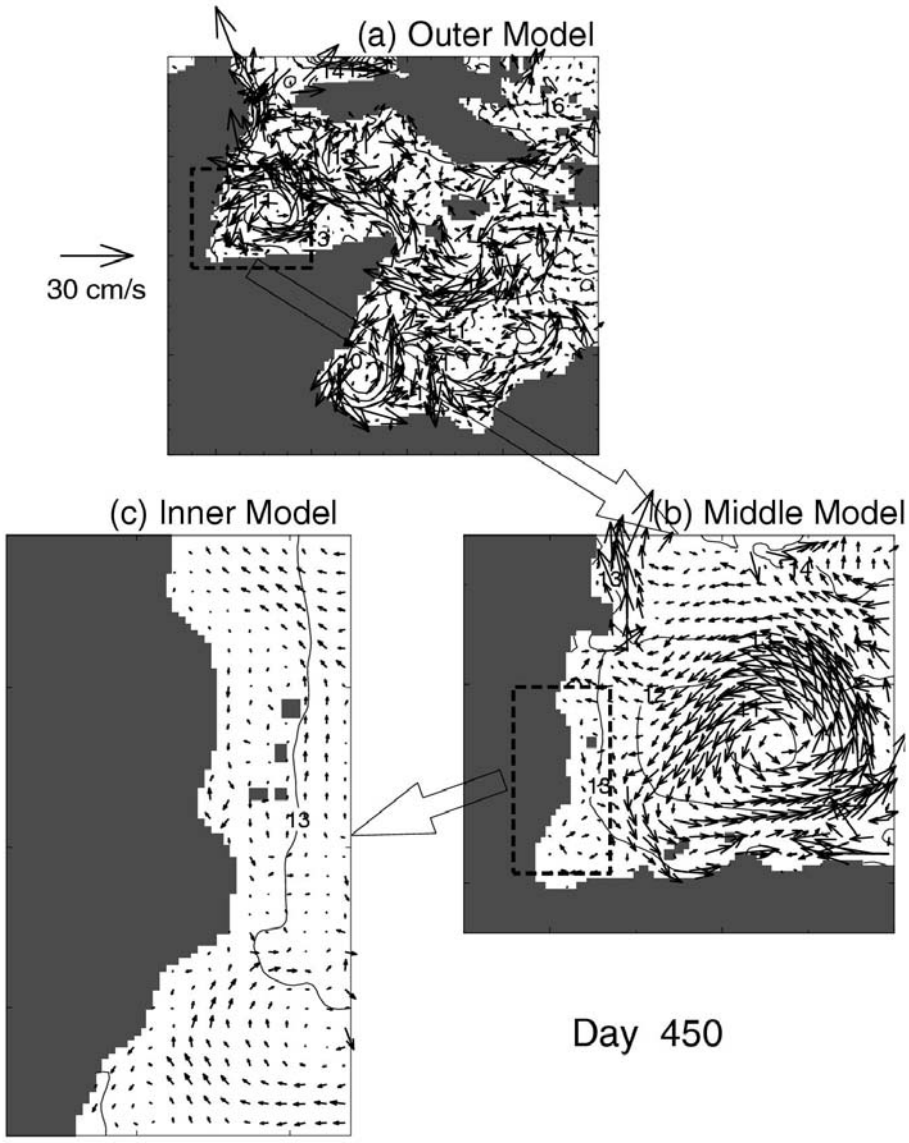

Figure 7. Sub-surface (450 m) currents and temperature at day 450 produced by the (a) outer model; (b) middle model, and (c) inner model. Velocity vectors are plotted at every third model grid point.

The main features of the monthly mean circulation produced by the outer model are in good agreement with those produced by Sheng and Tang (2003) using a single-domain model for the same region and climatological monthly mean wind forcing, and are also in good agreement with the current knowledge of the general circulation in the WCS (Maul, 1993; Mooers and Maul, 1998; Johns et al., 2002; Ezer et al., 2003; Ezer et al., 2005).

The monthly mean near-surface (1 m) temperatures produced by the outer model in the four months (now shown) are horizontally uniform in the central CS and about 25°C in February, 27°C in May and November, and 28°C in August. There is a pool of cold waters in the surface layer over the Campeche Bank off northern Yucatan Peninsula. This pool of cold waters is produced by the intense coastal upwelling occurring in the area. The monthly mean near-surface salinity in the four months is horizontally uniform in the central WCS, with relatively salty waters in the eastern Cayman and Yucatan Basins and fresh waters in the southern Yucatan Basin.

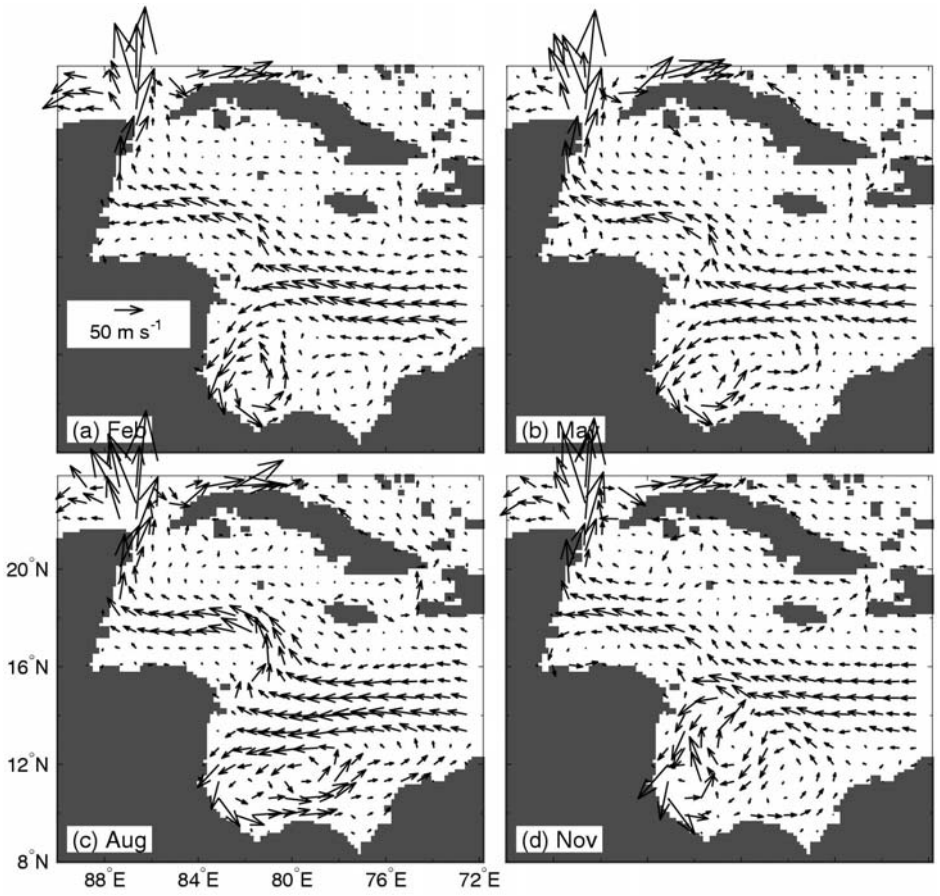

Figure 8. Monthly mean near-surface (1 m) currents calculated from 10-year results from 1991 to 2000 produced by the outer model in (a) February; (b) May; (c) August; and (d) November. Velocity vectors are plotted at every four model grid point.

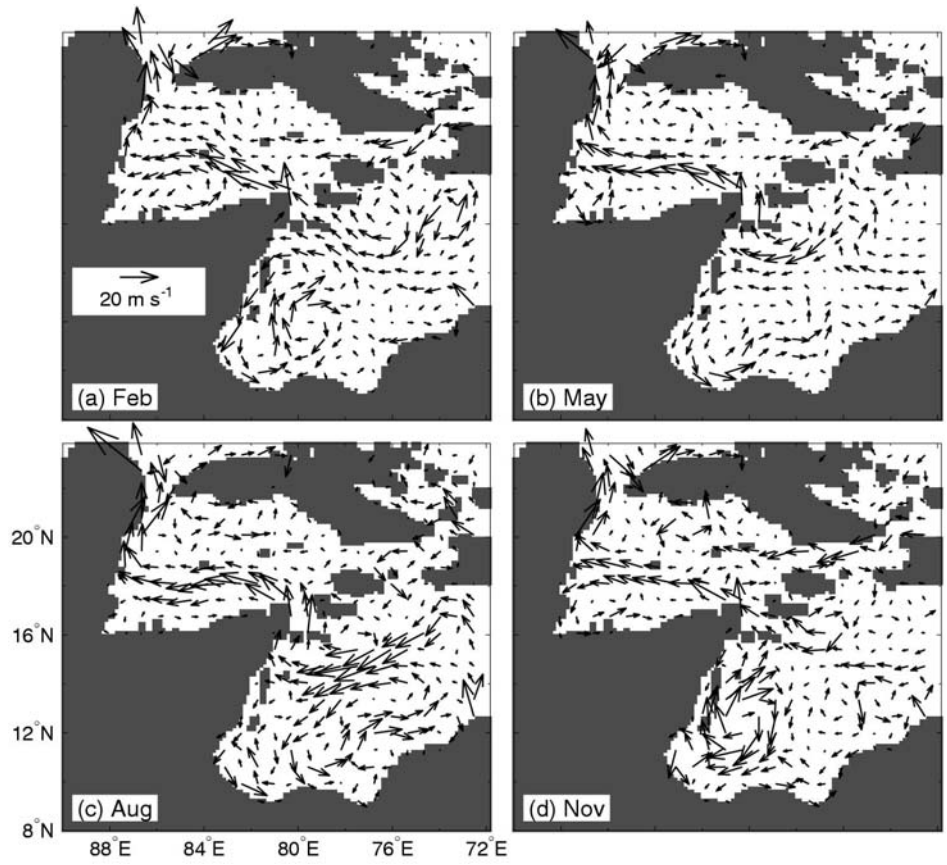

Figure 9. Monthly mean sub-surface (450 m) currents calculated from 10-year results from 1991 to 2000 produced by the outer model in (a) February; (b) May; (c) August; and (d) November. Velocity vectors are plotted at every four model grid point.

The sub-surface temperatures at 450 m have large seasonal variability, with relatively stronger cross-shelf gradients over the western sides of Cayman and Yucatan Basins in August than in February (Figures 10). In comparison with the temperature climatology, the model results maintain reasonably well the horizontal gradients of the sub-surface temperature in the region, particularly over the western Cayman and Yucatan Basins.

The 3D temperature and salinity produced by the outer model are used to calculate the domain-averaged temperature and salinity and associated standard deviations with respect to the domain means at each depth in the four months (Figure 11). In comparison with the climatological hydrographic data in Figure 5, the outer model reproduces reasonably well the vertical structure of the domain-averaged temperature and associated horizontal variations in the WCS. The outer model also reproduces reasonably well the vertical structure of the domain-averaged salinity

and associated horizontal variations at depths greater than 1000 m, but less well in the top 1000 m. Plausible explanations for the model deficiency in simulating the domain-averaged salinity in the top 1000 m include the application of the restoring boundary conditions for the surface salinity and simple vertical mixing parameterizations used in the model.

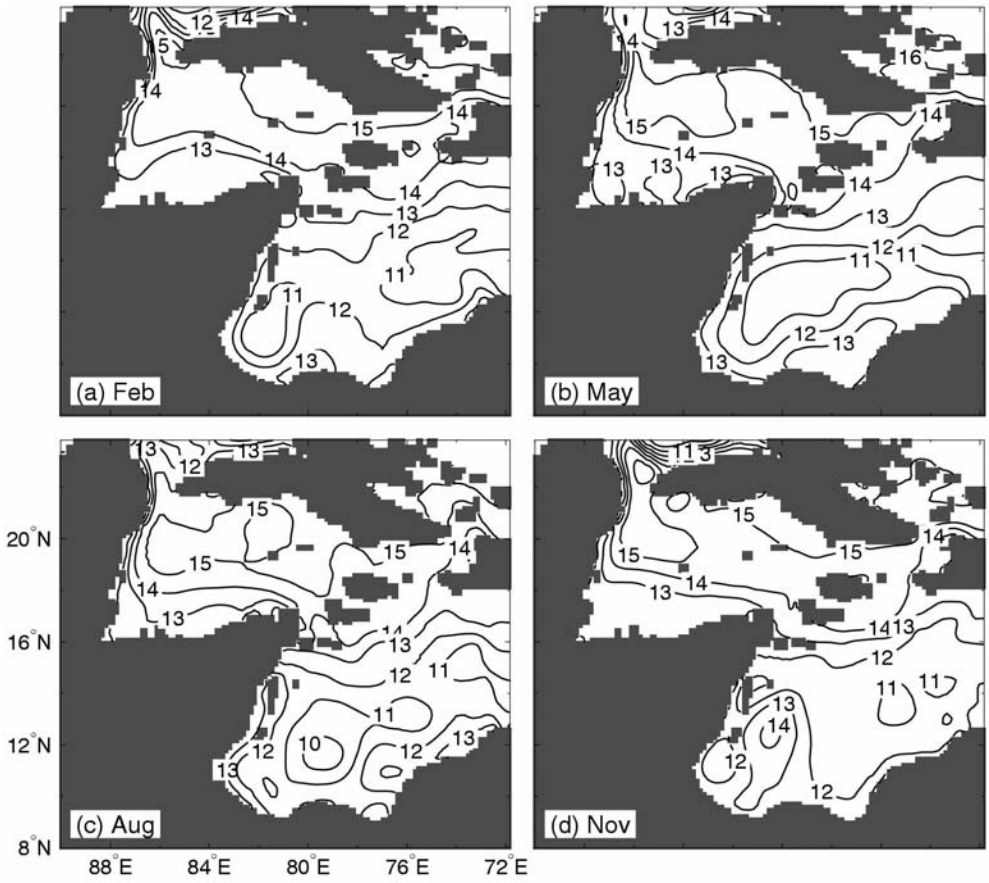

Figure10. Monthly mean sub-surface (450 m) temperature calculated from 10-year results from 1991 to 2000 produced by the outer model.

To quantify the temporal variability of the circulation in the WCS, I follow Sheng and Tang (2003) and calculate the root-mean-square (rms) values of $\sigma_{|u|}$ (= $(\sigma_u^2 + \sigma_v^2)^{1/2}$) at each grid point from the 10-year model results. Here σ_u and σ_v are respectively the rms values of the eastward and northward components of the currents with respect to the decadal means. Figure 12a demonstrates that the temporal variabilities of the near-surface currents produced by the outer model are large in the WCS, particularly over the southwestern Colombian Basin, with

a maximum value of $\sigma_{|u|}$ of about 18 cm s^{-1}. The large rms values over the southern Colombian Basin are associated mainly with the highly variable Panama-Colombian Gyre. The rms values of the near-surface currents are also large over the MBRS, with a maximum value of $\sigma_{|u|}$ of about 12 cm s^{-1}, indicating that the Caribbean Current has significant temporal variability over the region. In comparison with the near-surface results, the rms values of sub-surface currents at 140 m (Figure 12b) are relatively smaller, but still significant particularly over the southwestern Colombian Basin and MBRS region. The typical rms values of the sub-surface currents are about 6 cm s^{-1} over the MBRS and about 10 cm s^{-1} over the southwestern Colombian Basin.

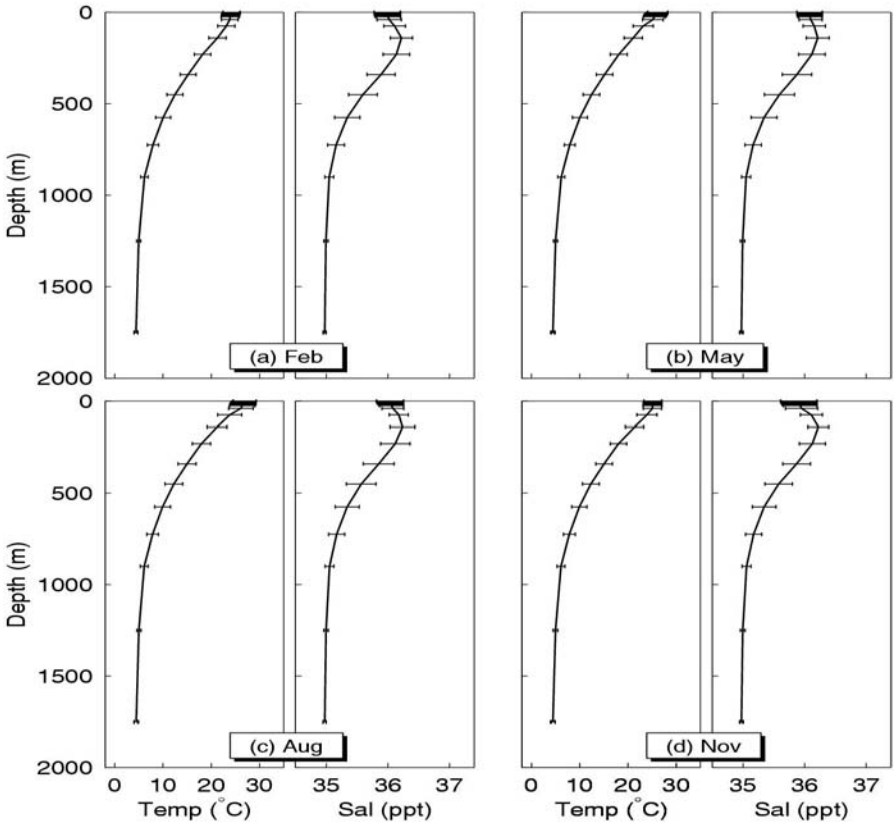

Figure 11. Vertical profiles of domain-averaged monthly mean temperature and salinity produced by the outer model in (a) February; (b) May; (c) August; and (d) November. The error bar represents 2 standard deviations with respect to the domain mean at each depth.

To assess the performance of the nested-grid system, the decadal mean currents at 16 m produced by the outer and middle models are compared with the decadal-mean

currents inferred by Fratantoni (2001) from trajectories of the satellite-tracked 15-m drogued drifters made during the 1990s (Figure 13). The nested-grid outer model reproduces reasonably well the large-scale features of the observed currents in the WCS, including the persistent Caribbean Current and the intense Panama-Colombia Gyre (Figure 13a). The middle model results also reproduce reasonably well the observed currents in the southern MBRS.

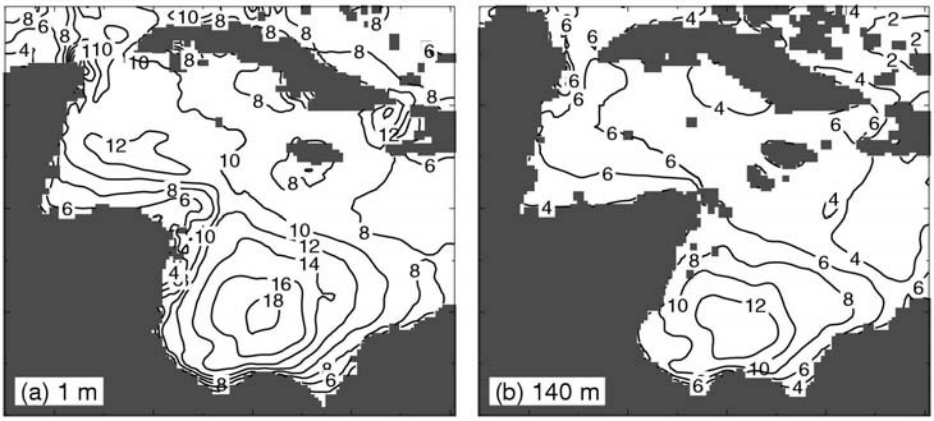

Figure 12. The root-mean-square values of $\sigma_{|u|}$ (in units of cm s^{-1}) of model currents at (a) 1 m; and (b) 140 m calculated from 10-year results produced by the outer model.

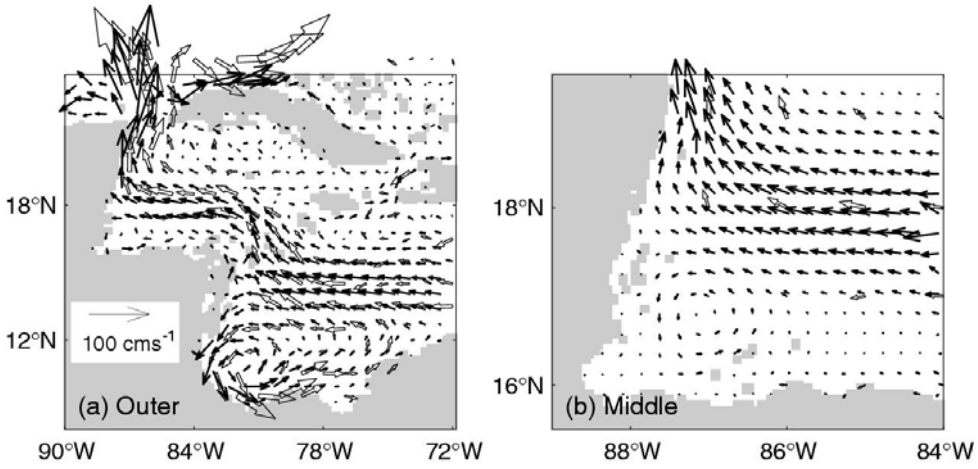

Figure 13. Comparison of modeled (solid arrows) and observed (open arrows) currents (a) in the WCS and (b) in the MBRS. The modeled currents are the decadal mean currents at 16 m produced by the nested-grid outer and middle models respectively. The observed currents are the gridded decadal mean currents during the 1990s inferred from trajectories by Fratantoni (2001).

Summary and conclusion

A triply nested-grid ocean modeling system was used to study the three-dimensional ocean circulation and water mass distributions on the Meso-American Barrier Reef System (MBRS) of the northwestern Caribbean Sea. The two-way nesting technique based on the smoothed semi-prognostic method (Sheng et al., 2005) was used to exchange information between sub-components of the system. The main advantage of this nesting technique is that it prevents unrealistic drift of the middle and inner models by adjusting large-scale circulations produced by the two models using the outer and middle model results, respectively, while the model temperature and salinity of the nested-grid model are fully prognostic.

The nested-grid system was forced by the 6-hourly NCEP wind forcing and monthly mean sea surface heat and freshwater fluxes. The system simulates reasonably well the general circulation in the WCS during the 10-year period from 1991 to 2000. The monthly mean near-surface circulation in the MBRS produced by the system is characterized by a strong and persistent northwestward flow over the MBRS, as a direct result of the interaction between the strong, directional Caribbean Current, and weak, spatially variable currents in the southern and inner Belize shelf. The upper-ocean circulation produced by the system also has significant spatial and temporal variability over the MBRS.

Acknowledgments

The author wishes to thank Liang Wang, Liqun Tang, Kyoko Ohashi, and three reviewers for their useful suggestions and comments. This study was supported by NASA (NNG04GO90G) to USF (subcontract: #2500-1083-00-A), and the NSERC/MARTEC/MSC Industrial Research Chair.

References

Andrade, C. A., and E. D. Barton, Eddy development and motion in the Caribbean Sea, *J. Geophys. Res.*, **105**, 26191-26201, 2000.

Barnier, B., L. Siefridt, and P. Marchesiello, Thermal forcing for a global ocean circulation model using a three year climatology of ECMWF analysis, *J. Mar. Sys*., **6**, 363-380, 1995.

da Silva, A. M., C. C. Young, and S. Levitus, Atlas of surface marine data 1994, Volume 3, Anomalies of heat and momentum fluxes, NOAA Atlas NESDIS **8**, NOAA, Washington, DC, 413 pp., 1994.

Dietrich, D. E., Application of a modified Arakawa `a' grid ocean model having reduced numerical dispersion to the Gulf of Mexico circulation, *Dyn. Atmos. and Oceans*, **27**, 201-217, 1997.

Ezer, T., L-Y Oey, and H-C Lee, The variability of currents in the Yucatan Channel: analysis of results from a numerical model, *J. Geophys. Res.*, **108**, 3012, doi:10.1029/2002JC001509, 2003.

Ezer, T., D. V. Thattai, B. Kjerfve, and W. D. Heyman, On the variability of the flow along the Meso-American Barrier Reef System: a numerical model study of the influence of the Caribbean Curent and eddies, *Ocean Dynamics*, doi:10.1007/s10236-005-0033-2, 2005.

Fratantoni, D. F., North Atlantic surface circulation during the 1990's observed with satellite-tracked drifters, *J. Geophys. Res.*, **106,** 22067-22093, 2001.

Greatbatch, R. J., J. Sheng, C. Eden, L. Tang, X. Zhai, and J. Zhao, The semi-prognostic method, *Continental Shelf Res.*, **24**, 2149-2165, 2004.

Geshelin, Y., J. Sheng, and R. J. Greatbatch, Monthly mean climatologies on temperature and salinity in the western North Atlantic, Can. Tech. Rep. Hydrogr. Ocean. Sci. **153**, 62 pp, 1999.

Haney, R. L., Surface thermal boundary conditions for ocean circulation models, *J. Phys. Oceanogr*., **1**, 241-248, 1971.

Hubbell, S. P., A unifield theory of biogeography and relative species abundance and its application to tropical rain forests and coral reefs, *Coral Reefs*, **16**, S9-S21, 1997.

Johns, W. E., T. L. Townsend, D. M. Fratantoni, and W. D. Wilson, On the Atlantic inflow to the Caribbean Sea, *Deep-Sea Res*., **49A**, 211-243, 2002.

Kramer, P. A., and P. R. Kramer, Ecoregional conservation planning for the Mesoamerican Caribbean Reef, 140 pp., 2002.

Large, W. G., and S. Pond, Open ocean momentum flux measurements in moderate to strong winds. *J. Phys. Oceanogr.*, **11**, 324-336, 1981.

Large, W. G., J. C. McWilliams, and S. C. Doney, Oceanic vertical mixing: A review and a model with a nonlocal boundary layer parameterization, *Reviews of Geophysics*, **32**, 363-403, 1994.

Marchesiello, P., J. C. McWilliams, and A. Shchepetkin, Open boundary conditions for long-term integration of regional oceanic models, *Ocean Modeling*, **3**, 1-20, 2001.

Maul, G. A., ed., Climatic Change in the Intra-Americas Sea, United Nations Environment Programme, Edward Arnold, London, 389 pp., 1993.

Mooers, C. N. K., and G. A. Maul, Intra-Americas Sea circulation, coastal segment (3,W), *The Sea*, 11, John Wiley and Sons, 183-208, 1998.

Nystuen, J. A., and C. A. Andrade, Tracking mesoscale ocean features in the Caribbean Sea using Geosat Altimetry, J. Geophys. Res., **98**, 8389-8394, 1993.

Oey, L-Y, T. Ezer, and H-C Lee, Loop current, rings and related circulation in the Gulf of Mexico: a review of numerical models and future challenges, In *Ocean circulation in the Gulf of Mexico*, edited by W. Sturges and A. L. Fernandez, Geophys. Monograph/ Ser., AGU, Washington, DC, in press, 2005.

Orlanski, I., A simple boundary condition for unbounded hyperbolic flows, *J. Comput. Phys.*, **21**, 251-269, 1976.

Sou, T., G. Hollaway, and M. Eby, Effects of topographic stress on Caribbean Sea circulation, *J. Geophys. Res.*, **101**, 16449-16453, 1996.

Sheng, J., and L. Tang, A numerical study of circulation in the western Caribbean Sea, *J. Phys. Oceanogr.*, **33**, 2049-2069, 2003.

Sheng, J., and L. Tang, A two-way nested-grid ocean-circulation model for the Meso-American Barrier Reef System, *Ocean Dynamics*, **54**, 232-242, 2004.

Sheng, J., R. J. Greatbatch, and D. G. Wright, Improving the utility of ocean circulation models through adjustment of the momentum balance, *J. Geophys. Res.*, **106**, 16711-16728, 2001.

Sheng, J., R. J. Greatbatch, X. Zhai, and L. Tang, A new two-way nesting technique based on the smoothed semi-prognostic method, *Ocean Dynamics*, **55**, doi: 10.1007/s10236-005-00005-6, 162-177, 2005.

Sheng, J., D. G. Wright, R. J. Greatbatch, and D. E. Dietrich, CANDIE: A new version of the DieCAST ocean circulation model, *J. Atmos. and Ocean. Tech.*, **15**, 1414-1432, 1998.

Smagorinsky, J., General circulation experiments with the primitive equation. I. The basic experiment, *Mon. Wea. Rev.*, **21**, 99-165, 1963.

Tang, L., J. Sheng, J., B. G. Hatcher, and P. F. Sale, Numerical study of circulation, dispersion and hydrodynamic connectivity of surface waters on the Belize shelf, *J. Geophys. Res.*, **111**, C01003, doi:10.1029/2005JC002930, 2006.

Thuburn, J., 1996: Multidimensional flux-limited advection schemes, *J. of Comput. Phys.*, **123**, 74-83, 1996.